

Outer Sphere Adsorption of Pb(II)EDTA on Goethite*

John R. Bargar^{1,**}, Per Persson², and Gordon E. Brown, Jr.^{1,3}

Abstract

FTIR and EXAFS spectroscopic measurements were performed on Pb(II)EDTA adsorbed on goethite as functions of pH (4-6), Pb(II)EDTA concentration (0.11 μM - 72 μM), and ionic strength (16 μM - 0.5M). FTIR measurements show no evidence for carboxylate-Fe(III) bonding or protonation of EDTA at Pb:EDTA = 1:1. Both FTIR and EXAFS measurements suggest that EDTA acts as a hexadentate ligand, with all four of its carboxylate and both amine groups bonded to Pb(II). No evidence was observed for inner-sphere Pb(II)-goethite bonding at Pb:EDTA = 1:1. Hence, the adsorbed complexes should have composition Pb(II)EDTA²⁻. Since substantial uptake of PbEDTA(II)²⁻ occurred in the samples, we infer that Pb(II)EDTA²⁻ adsorbed as outer-sphere complexes and/or as complexes that lose part of their solvation shells and hydrogen bond directly to goethite surface sites. We propose the term "hydration-sphere" for the latter type of complexes because they should occupy space in the primary hydration spheres of goethite surface functional groups, and to distinguish this mode of sorption from common structural definitions of inner- and outer-sphere complexes. The similarity of Pb(II) uptake isotherms to those of other divalent metal ions complexed by EDTA suggests that they too adsorb by these mechanisms. The lack of evidence for inner-sphere EDTA-Fe(III) bonding suggests that previously proposed metal-ligand - promoted dissolution mechanisms should be modified, specifically to account for the presence of outer-sphere precursor species.

Submitted to Geochimica et Cosmochimica Acta

¹Stanford Synchrotron Radiation Laboratory, PO Box 4349, Stanford, CA, 94309, bargar@slac.stanford.edu;

²Dept. of Inorganic Chemistry, Umeå University, Umeå, S-901 87 Sweden, per.persson@chem.umu.se;

³Dept. of Geological and Environmental Sciences, Stanford University, Stanford, CA, 94305-2115, gordon@pangea.stanford.edu.

**Corresponding author.

1. INTRODUCTION

Pb(II) and EDTA are common, toxic contaminants in surface and ground waters, and their transport, toxicity, and bioavailability are heavily impacted by ternary (and higher order) interactions with water, each other, and oxide and (oxy)hydroxide surfaces. Pb(II) contamination is ubiquitous, arising from mine wastes, leakage of paint and combustion of leaded fuels, and industrial activities such as smelting. EDTA is a common constituent of household products and industrial processes, typically entering the environment *via* discharge of sewage effluent to natural waters (Means et al., 1980). Once present in the subsurface, EDTA is slow to degrade (Means, 1980; Kari and Giger, 1995). Due to its tendency to chelate metal ions, it induces long-lived perturbations of metal ion speciation in the subsurface. Pb(II) and EDTA each adsorb strongly on oxide surfaces (Jenne, 1967; Hem 1976; Erel and Morgan, 1992; Jardine *et al.* 1993; Szecsody *et al.*, 1994; Nowack and Sigg, 1996, 1997, and references therein). When mutually present, EDTA may complex Pb(II) and strongly affect its adsorptive behavior. For example, addition of EDTA to lead-contaminated soils dramatically increases the bioavailability of Pb(II) to plants, presumably due to liberation of adsorbed Pb(II) from mineral surfaces and solid phases (Jørgensen, 1993; Huang *et al* 1996, 1997; Blaylock *et al*, 1997). The speciation of Pb(II)EDTA and EDTA in sub-surface environments is also impacted by dissolution of Fe-oxides and the subsequent formation of aqueous and adsorbed Fe(III)EDTA complexes. Several authors have proposed that Pb(II) and EDTA co-adsorb on oxides as ternary complexes (Bowers and Huang, 1986; Girvin *et al.* 1993; Jardine *et al.*, 1993; Szecsody *et al.*, 1994; Zachara *et al.*, 1995; Nowack and Sigg, 1996, 1997). Both inner- and outer-sphere models have been proposed. The actual mechanism has been difficult to assign. The extent of Pb(II)EDTA uptake is dependent on ionic strength at near- and sub-neutral pHs (Nowack and Sigg, 1996), suggesting predominantly electrostatic sorption. However, Pb(II)EDTA also exhibits weak but finite uptake on Fe- and Al-oxides at $\text{pH} \cdot \text{pH}_{\text{pzc}}$ (Bowers and Huang 1986; Nowack and Sigg, 1996), suggesting the existence of non-electrostatic bonding forces. It is of practical importance to distinguish between these modes of sorption because the distance of approach and type of bonding of ions to oxide surfaces heavily influence the adsorbing ion's chemical properties and reactivity (Stumm, 1992). Fundamental knowledge regarding the reaction rates and stoichiometries of any of the components of such systems would also be of great use in modeling Pb(II) and EDTA mobility under the dynamic chemical conditions of aquifers and would improve our ability to design remediation strategies.

The primary objectives of this study were to define the modes of sorption (inner vs. outer-sphere), and the molecular structures, compositions, and reaction stoichiometries of Pb(II)EDTA ternary complexes on goethite using extended x-ray absorption fine structure (EXAFS) and Fourier transform infrared (FTIR) spectroscopic measurements. Little is known about these defining aspects or about the molecular transformations occurring between Pb(II)EDTA adsorption and Fe-oxide dissolution. FTIR measurements directly probe vibrations of the EDTA molecule, which are highly sensitive to its structure, protonation state, and coordination environment. Both diffuse reflectance (DR-FTIR) and attenuated total reflectance (ATR-FTIR) measurements were performed in this study. EXAFS measurements provide quantitative information about molecular structure from the perspective of Pb(II). Goethite (α -FeOOH) is a common mineral in soils, surface waters, and aquifers, and has large sorptive capacities for both Pb(II) and EDTA (Gunneriusson *et al.*, 1994; Nowack and Sigg, 1996).

This study is an extension of our EXAFS and FTIR measurements of Pb(II) and carboxylate adsorption, on Al- and Fe-oxides (Bargar *et al.*, 1996; 1997a,b,c,d; 1998; 1999; Nordin *et al.*, 1997; 1998; Persson *et al.*, 1998a,b). The results of the current study suggest that Pb(II)EDTA²⁻ adsorbs primarily as outer-sphere ions and/or *via* direct hydrogen bonds to surface functional groups, which displace part of the aqueous solvation shell.

1.1 Previous Work

Bowers and Huang (1986) studied electrophoretic mobility and metal ion uptake of divalent metal ion-EDTA complexes on γ -Al₂O₃. They observed (1) a weak surface charge reversal in the presence of Ni(II)EDTA, (2) ligand-like uptake of Pb(II)EDTA and Ni(II)EDTA, both extending to $\text{pH} \cdot \text{pH}_{\text{pzc}}$, (3) a relative independence of Me(II)EDTA uptake on the identity of Me(II), and (4) a correlation between Me(II)EDTA adsorption density and the inferred density of AlOH₂⁺ surface functional groups. Based on these observations, the authors concluded that Me(II)EDTA complexes adsorbed *via* hydrogen-bonding ion-pair formation with AlOH₂⁺ groups; however, they offered no molecular model of the hydrogen-bonding interactions. Girvin *et al.* (1993) studied the pH dependence of Co(II) and Co(III) uptake on γ -Al₂O₃ in 0.1 to 0.001M M NaClO₄. They proposed that free carboxylate groups (*i.e.*, not bonded to Co) of quinquedentate Co(II)/(III)EDTA complexes (*i.e.*, 3 carboxylate and 2 amine groups bonded to Co(II)) hydrogen bond to surface hydroxyls, and that carboxylate-surface hydrogen bonding may also occur for fully coordinated hexidentate complexes.

Szecsody *et al.* (1994) measured Co(II)EDTA sorption on Fe-coated sand and Fe(III) release over a variety of reaction times. Bryce *et al.* (1994) found that EDTA and Ni(II)EDTA sorption on ferrihydrite is fast (occurring in minutes) and that Ni(II) adsorption occurs faster than the formation of Ni(II)EDTA solution complexes. Zachara *et al.* (1995) found that, at pH • 5, Co(II)EDTA adsorption on goethite and aquifer sands is followed by significant Co(II)EDTA dissociation within 30 minutes. Nowack and Sigg (1996, 1997) studied Me(II)- and Me(III)-EDTA uptake on goethite and metal-ligand promoted dissolution of goethite and ferrihydrite. Their results show that Pb(II)EDTA uptake is weak but positive at pH > pH_{pzc}, and that it is ionic-strength dependent. They proposed a Me(II)EDTA-promoted dissolution model in which quinquedentate Me(II)EDTA complexes bond to surface ≡Fe sites and then transform into an activated complex having EDTA simultaneously bonded to Fe(III) and Me(II) as tridentate iminodiacetic ligands.

XAFS investigations of Pb(II) sorption on Al- and Fe-oxides and -(oxy)hydroxides in the absence of strongly complexing ligands have been performed by several groups (Chisholm-Brause *et al.*, 1990; Roe *et al.*, 1991; Manceau *et al.*, 1992; Bargar *et al.*, 1996; 1997a,b,d; 1998). These studies show that Pb(II) ions adsorb on Al- and Fe-oxides preferentially as fully hydrolyzed, mononuclear complexes that are bonded to edges of surface AlO₆ or FeO₆ octahedra in bidentate and/or tridentate fashions. EDTA has four carboxylate groups that, in principle, can bond to Pb(II) and/or Fe(III). FTIR investigations of carboxylate adsorption on Al- and Fe-oxides and -(oxy)hydroxides have shown that carboxylates can adsorb as inner-sphere and outer-sphere surface complexes. The mode of coordination to the surface has been shown to be sensitive to factors such as the composition and structure of the ligand, pH, and ionic strength (Nordin *et al.*, 1997; Nordin *et al.*, 1998; Persson *et al.*, 1998a; Persson *et al.*, 1998b). For outer-sphere complexes, the most negatively charged (fully ionized) form of the ligand (L⁴⁻) was found to be stabilized at the interface.

2. MATERIALS and METHODS

2.1 Materials

Goethite (45 m²/g, pH_{pzc} = 8.9 in absence of CO₂) was supplied by Alexander Robertson, Department of Civil and Environmental Engineering, Stanford University, and was synthesized according to the procedure described in Van Geen *et al.* (1994). XPS analyses of the powders showed the surfaces to have only Fe, O, and

adventitious carbon. FTIR measurements in this study showed no trace of NO_3^- , SO_4^{2-} , or ClO_4^- impurities. Regional and full powder XRD scans showed no extra peaks attributable to other Fe-oxides.

2.2 FTIR Sample Preparation, Measurement, and Analysis

All solutions were prepared from Milli-Q water boiled under N_2 to remove CO_2 . Goethite stock suspensions (5.5 g/L) were adjusted to pH 4 with 0.7 mM HCl and sparged with Ar overnight to remove CO_2 and help disperse goethite. Suspensions were stirred with Teflon-coated stir bars, and water-saturated Ar was bubbled through samples during all pH measurements and adjustments. Aliquots of goethite stock suspension were added to 20 mL (DR-FTIR) or 50 mL (ATR-FTIR) polycarbonate centrifuge tubes and adjusted to the approximate final pH with NaOH or HCl. Samples were wrapped in Al foil, aliquots of 1:1 Pb(II)EDTA solution (as PbCl_2 and $\text{Na}_2\text{EDTAH}_2$) were added, and pH was readjusted to the target value. Typically, pHs stabilized within 30 seconds of pH adjustment and did not change thereafter over a 24-hour time interval. Samples were rotated end-over-end for 15 - 24 hrs. before FTIR measurements.

Following end-over-end rotation, samples were centrifuged for 15 - 45 min. at 2,000xg to 19,000xg, RCF to concentrate the solid. $\geq 99.5\%$ (by mass) of the supernatant could thus be removed. Based on 48% - 99% uptake, surface-bound Pb(II)EDTA was in excess of dissolved EDTA by factors ≥ 100 . Dissolved Pb(II) was measured by graphite-furnace atomic absorption (GFAA) spectrometry. Supernatants were filtered (0.45 μm cellulose Millipore membranes) prior to GFAA analysis. Results are given in Table 1.

FTIR spectra were collected using a Perkin-Elmer 2000 spectrometer (4 cm^{-1} resolution, mirror velocity of 1 $\text{cm}^{-1}/\text{sec.}$), Harrick diffuse reflectance accessory (deuterated triglycine sulfate detector) (DR-FTIR measurements) and a horizontal Amtir ATR assembly (45° incidence angle) with a mercury-cadmium-telluride detector. 500 scans (DR-FTIR) or 4,000 scans (ATR-FTIR) were measured for each sample. DR-FTIR analysis: centrifuged samples were placed on filter membranes (Schleicher & Schuell, membranfilter® 0.025 μm) in an Ar-filled desiccator for approximately 25 min. to remove water by capillary action. To verify that evaporative desiccation did not occur, a piece of polypropylene film was placed over the open (exposed) side of test wet paste-on-filter samples to prevent evaporation. These samples became desiccated to the same level as the others in about 25 min. The presence of water peaks in DR-FTIR spectra (prior to background subtraction) indicated that some water remained on the surfaces following this procedure. 10 mg of sample were gently mixed with 0.5 gm of preground KBr and loaded into DR-FTIR sample holders. Previous studies (Bargar et al., 1999) suggest that dispersal in KBr should not perturb adsorbate speciation. The spectrum of clean goethite (pH 4) was subtracted

from sample spectra (subtraction factors ranged between 0.95 and 1.05; 1.0 is expected for perfectly measured and mixed samples) to remove bulk goethite peaks. The similarity of DR- and ATR-FTIR sample spectra presented herein suggest that DR-FTIR sample preparation procedures did not perturb Pb(II)EDTA adsorbate speciation. ATR-FTIR analysis: wet centrifuged Pb(II)EDTA-reacted goethite was spread over the ATR crystal to a thickness of 1 to 2 mm, over which was placed several mL of supernatant. Water-saturated Ar was maintained over samples during data collection. Supernatant and clean goethite spectra were subtracted from sample spectra to remove peaks from bulk water, aqueous complexes, and bulk goethite.

2.4 XAFS Sample Preparation, Measurement, and Analysis

Samples were prepared in 65 mL polycarbonate centrifuge tubes under N_2 atmosphere in batch mode similar to ATR- and DR-FTIR samples (Table 2). Prior to addition of Pb(II), goethite suspensions were sparged with N_2 for 20 minutes at pH 3 (adjusted with 1 mM HNO_3) to remove adsorbed CO_2 and helped disperse the goethite. Pb(II)EDTA stock solution (25 mM $Pb(NO_3)_2$ in 25 mM Na_2EDTAH_2) was added to samples while they were vigorously stirred. After adjustment the target pH, samples were rotated end-over-end for 36 - 60 hr. and centrifuged (17,150 g at 21° C for 15 min.). We have detected no effect of electrolyte type on the adsorbed species (*cf.*, section 3.1). Typically, > 99.5% of the supernatant was removed. Hence, surface-bound Pb(II)EDTA exceeded dissolved EDTA by 35x to 1,800x. Pb L_{III}-edge EXAFS fluorescence data were collected at room temperature at SSRL BL 4-3 using a Lytle-type detector. Data collection parameters were: silicon (220) double-crystal monochromator (approximately 6.4 eV FWHM resolution) detuned 35%, 2x20 mm beam size defined by Ta slits. An As 6- μ x filter and Al foils were used as fluorescent x-ray filters. The second inflection point of the Pb foil edge-jump was set to 13,055 eV.

EXAFS spectra were background-subtracted, spline-fit, k^3 -weighted and quantitatively analyzed in k -space using the EXAFSPAK software (George, 1993) following procedures described in Bargar *et al.* (1997a,b). Backscattering phase and amplitude functions required for numerical fitting of spectra were obtained from XAFS of well-characterized, crystalline model compounds and FEFF 6 calculations ($S_0^2=1$, $exch=1,3$, $Ion=0$) (Rehr and Albers, 1990; Rehr *et al.*, 1991; 1992). The full structure out to 6 Å was used as FEFF input to obtain correct potentials. Pb-O and Pb-C bond distances ($R_{Pb-O, Pb-C}$) and corresponding coordination numbers (CNs) were found to be accurate to ± 0.03 Å, $\pm 20\%$, respectively, based on fits to model compounds (Bargar *et al.*, 1997a; Bargar *et al.*, 1998). A single value of E_0 was varied for all shells. Second- and third-shell Debye-Waller (σ^2) values were initially allowed to vary during fitting. Second-shell (Pb-C) σ^2 values were found to cluster around 0.013 Å²

and henceforward were fixed to this value. Third-shell (Pb-O) σ^2 values were fixed at 0.012 Å² for the same reason. Parameters allowed to float in fits were: $R_{\text{Pb-O}}$, $R_{\text{Pb-C}}$, $R_{\text{Pb-N}}$, $\text{CN}_{\text{Pb-O}}$, $\text{CN}_{\text{Pb-C}}$, and $\sigma_{\text{Pb-O}}^2$.

3. RESULTS

3.1 FTIR Spectra of Pb(II)EDTA Adsorbed on Goethite

FTIR spectra of the Pb(II)EDTA/goethite samples are presented in Figs. 2 - 4. The C-O stretching frequencies of the carboxylate groups on the EDTA molecule (about 1350 - 1650 cm⁻¹) are relatively intense, sensitive to the ionization and coordination states of the molecule, and thus can be used to deduce the structures of EDTA complexes (Nakamoto, 1986). The most intense carboxylate IR absorption peak in this region is the asymmetric C-O stretching frequency, denoted in this paper as ν_{asym} (•1600 cm⁻¹ in Figs. 2-4), which can have values ranging from about 1550 cm⁻¹ to about 1650 cm⁻¹, depending upon the coordination of the EDTA molecule (Nakamoto, 1986). Carboxylate-Pb(II) and -Fe(III) bonding, produce C-O ν_{asym} values of 1570 to 1600 cm⁻¹ (Sawer and Tacket, 1963; Reed and Kula, 1971; McConnell and Nuttall, 1977; Nakamoto, 1986; Rojo *et al.*, 1992; Yugeng, 1993, and this paper), and 1610 to 1696 cm⁻¹ (Busch and J.C. Bailar, 1953; Morris and Busch, 1956; Fujita *et al.*, 1962; Sievers and J.C. Bailar, 1962; Scott *et al.*, 1973; Nakamoto, 1986), respectively (Fig. 2). In both cases, the intensities of C-O ν_{asym} are proportional to the number of EDTA carboxylate groups bonded to the given metal ion (Nakamoto *et al.*, 1963). Peaks occurring between about 1350 and 1450 cm⁻¹ belong to the C-O symmetric stretching frequency (ν_{sym}). Their shapes and positions are also sensitive to the coordination state of EDTA, and their qualitative comparison provides another means to infer the structures and bonding of EDTA molecules.

ATR-FTIR spectra of Pb(II)EDTA/goethite (0.1M M NaCl) as a function of pH are presented in Fig. 2. The energy positions of C-O ν_{asym} in the sorption sample spectra (1569 cm⁻¹) are consistent with ν_{asym} energy values for carboxylate groups bonded to Pb(II). In contrast, C-O ν_{asym} occurs at 1609 cm⁻¹ for Fe(III)EDTA⁻(aq), and 1617 cm⁻¹ for H₂EDTA²⁻, which should be the stable form of uncomplexed aqueous EDTA between pH 4 and 6. There are no distinguishable Fe(III)-bonded EDTA peak contributions to C-O ν_{asym} in the sorption sample spectra. To illustrate this point, the C-O ν_{asym} peak in the pH 6 sample was fit with a Gaussian/Lorentzian lineshape (for which $\chi^2 = 0.00002790 \text{ abs}^2$) over the energy range 1500 to 1631 cm⁻¹ (Fig. 2). Comparison of this fit to the sample spectrum shows little evidence for amplitude at

1609 cm^{-1} . When a carboxylate-Fe(III) peak was forced to be present 1609 cm^{-1} in the fits, and its height and width were allowed to vary, the resultant feature accounted for less than 0.2% of the total peak area, and the overall fit quality improved by an insignificant amount ($\chi^2 = 0.00002789 \text{ abs}^2$). Furthermore, the C-O ν_{sym} regions of the spectrum closely match that of $\text{Pb(II)EDTA}^{2-}(\text{aq})$ and differ from the C-O ν_{asym} region of $\text{Fe(III)EDTA}^{-}(\text{aq})$. We conclude that carboxylate-Fe(III)-bonded EDTA species do not occur in the samples at detectable concentrations. Thus, the spectra suggest that the predominant adsorbate species are Pb(II)EDTA^{2-} chelate complexes electronically and structurally similar to $\text{Pb(II)EDTA}^{2-}(\text{aq})$.

To ascertain the extent to which Pb(II)EDTA adsorbate speciation was affected by sorption density, we measured spectra of Pb(II)EDTA /goethite at sorption densities ranging from 0.06 to 1 $\mu\text{mol./m}^2$. DR-FTIR spectra for these samples are presented in Fig. 3 (ATR-FTIR measurements lacked sufficient sensitivity to be used at the lowest of these sorption densities). The position of the C-O ν_{asym} peak in all spectra suggests that EDTA carboxylate groups are bonded to Pb(II). Based on the results of Bargar *et al.*, (1999), we ascribe the slight shifting of the DR-FTIR C-O ν_{asym} to higher frequency with increasing sorption density to a decrease in inter-particle spacing allowed by decreasing surface charge, which reduces the inter-particle water content in the DR-FTIR samples. This tenet is supported by the suspension properties of the goethite, which flocculated quickly in the 0.98 $\mu\text{mol./m}^2$ sample but very slowly at 0.06 $\mu\text{mol./m}^2$, and by the observation that C-O ν_{asym} in the lowest-sorption-density DR sample occurs at the same frequency as in ATR-FTIR spectra. The C-O ν_{asym} peaks are symmetric and show no evidence for any shoulder at 1610 cm^{-1} , indicating that Fe(III)-bonded carboxylate groups were not present at detectable concentrations. Furthermore, the C-O ν_{sym} regions of the spectra are similar to that of $\text{Pb(II)EDTA}^{2-}(\text{aq})$ and different from that of $\text{Fe(III)EDTA}^{-}(\text{aq})$. Thus, we conclude that non-inner-sphere Pb(II)EDTA^{2-} complexes predominated at all sorption densities studied.

Figure 4 shows the effect of ionic strength on the Pb(II)EDTA /goethite spectra. The spectra indicate the presence of carboxylate groups bonded to Pb(II) and contain no discernible evidence for carboxylate bonding to Fe(III). Spectra from samples prepared in NaNO_3 and NaClO_4 are also presented in Fig. 4. The peak positions are similar to the other spectra, suggesting Pb(II)EDTA adsorbate speciation is not significantly affected by the composition of the electrolyte medium in these measurements.

3.2 EXAFS Spectra of Pb(II)EDTA Adsorbed on Goethite

EXAFS spectra of Pb(II)EDTA/goethite were measured to characterize the structures and coordination environment of adsorbate species from the perspective of the metal ion. Spectra were recorded at pH 5 for the purposes of measuring adsorbate species at conditions of sufficiently high uptake, necessary to collect usable data, in the presence and absence of EDTA (Fig. 5). EXAFS fitting results are presented in Table 2. All Pb(II)EDTA/goethite sorption sample EXAFS spectra and FTs closely resemble those of Pb(II)EDTA²⁻ (aq) and differ substantially from those of Pb(II) on goethite in the absence of EDTA (*cf.*, Fig. 5). Pb L_{III}-edge EXAFS spectra are highly sensitive to the local Pb coordination environment, hence these observations suggest that the predominant Pb(II)EDTA adsorbate species on goethite are Pb(II)EDTA²⁻ chelate complexes, in agreement with the FTIR results. The spectrum from the sample having an excess of Pb(II) (Pb:EDTA = 2:1) can be fit (Fig. 5) using a linear combination of the spectra from the $\Gamma = 1.8 \mu\text{mol./m}^2$ Pb(II)EDTA/goethite sample and Pb(II) adsorbed on goethite as an inner-sphere complex. This observation suggests that excess Pb(II) adsorbs on goethite as inner-sphere complexes.

3.3 Pb(II) 1st Coordination Shell

Vibrational spectroscopy (Krishnan and Plane, 1968) and crystal structures (van Remoortere *et al.*, 1971; Shields *et al.*, 1973; Harrison *et al.*, 1982; Harrison and Steel, 1982) of Pb(II)EDTA and Sn(II)EDTA complexes indicate that the first coordination shell should contain two N atoms at distances similar to first-shell O atoms. EXAFS contributions from O and N are sufficiently similar that it is often not possible to distinguish between them in unconstrained fits to spectra (accordingly, we refer to the mixed first-shell as O/N). However, for this reason, if the N shell were neglected in fits to the Pb(II)EDTA spectra, the fit-derived values of the N coordination number ($\text{CN}_{\text{Pb-O}}$) were found to increase by about two (from about 4 to about 6 O atoms), and the Pb-N distance ($R_{\text{Pb-O}}$) decreased by about 0.02 Å, with little change in the quality of fit. Exclusion of N from fits would not change our EXAFS-based interpretations, since the same number of O/N atoms at about the same distances would be obtained. Nevertheless, inclusion of N in the first shell should more closely approximate physical reality. Therefore, two N atoms were included in the first-shell fits reported in Table 2, with σ^2 constrained to have the values obtained for first-shell oxygens. FEFF 6-derived phase and amplitude parameters for N, C, and O in Pb(II)EDTA were derived from a model based on the crystal structure of Sn₂EDTAx2H₂O (van Remoortere *et al.*, 1971) (Fig. 6) because no reliable Pb(II)EDTA structures were available in the

literature, to our knowledge. Sn(II) is an excellent model for Pb(II) because the two ions have very similar coordination chemistries and radii (Sn(II) is 5% smaller than Pb(II)) (Greenwood and Earnshaw, 1985).

Fits to the sample spectra indicate that the inner-most parts of Pb(II) first coordination shells are composed of approximately 6 to 7 O/N atoms at distances ranging from 2.38 to 2.53 Å (Table 2). Bargar *et al* (1997a,c) pointed out that EXAFS-determined CNs for Pb(II) 1st shells, which are derived from the normalized EXAFS amplitudes may underestimate the true CN by up to 50% due to amplitude reducing effects. Therefore, the EXAFS-derived CNs and Pb-O/N distances suggest that the inner-most part of the Pb(II) 1st shell consists of 6 O/N, which we attribute to the 2 amine N and 4 carboxylate O atoms of EDTA. The full CN can be estimated from $R_{\text{Pb-O/N}}$ by comparing it to CN vs. $R_{\text{Pb-O}}$ trends observed in oxides, oxosalts, and hydrates (Bargar *et al*, 1997a). This approach works well because the average and minimum $R_{\text{Pb-O}}$ vary rapidly with CN (Fig. 7). Since the minimum $R_{\text{Pb-O/N}}$ in EXAFS samples ranges from 2.38 to 2.47 Å, the minimum $R_{\text{Pb-O}}$ curve in Fig. 7 suggests that the true CN for Pb(II)EDTA first-shells is 7 to 8 O/N atoms. The 7th and 8th O atoms are most likely water molecules, the distances of which may be estimated from the average $R_{\text{Pb-O}}$ curve in Fig. 7, yielding $R_{\text{Pb-OH}_2} \approx 3.3$ Å. This result is consistent with the structures of Sn(II)EDTA complexes in crystals (van Remoortere *et al.*, 1971; Shields *et al.*, 1973; Harrison *et al.*, 1982; Harrison and Steel, 1982), which suggests that the electron lone pairs are stereochemically active, preventing the close approach of ligands external to the EDTA molecule (*i.e.*, < 2.75 Å).

3.4 Pb(II) 2nd Coordination Shell

The Pb(II)EDTA sorption sample and aqueous solution spectra contain strong second frequencies, manifest in the FTs (Fig. 5) as peaks at *ca* 2.7 Å (uncorrected for phase shift). Fits to the spectra indicate the Pb(II)-second shell distance is 3.20 to 3.30 Å, depending upon whether the backscatter is O, N or C. This distance corresponds closely to expected distances to C neighbors, of which there are many (up to 10). In Sn(II)EDTA (Fig. 6), Sn-C distances are 3.11, 3.21, 3.22, 3.23, 3.26, 2x3.27, 3.32, 3.36, and 3.46 Å. Hence, the 2nd-shell peak of our EXAFS samples can be interpreted in terms of Pb-C single scattering (SS). This assignment is supported by the excellent fits provided by a single shell of C atoms (Fig. 5). To ascertain whether the 2nd-shell FT peak could arise from multiple scattering (MS), we conducted FEFF 6 calculations on the structure shown in Fig. 6. Only two MS paths have distances in the relevant range (< 3.5 Å). Both are triangular Pb-C-O-Pb paths (effective path

lengths of 3.3 to 3.4 Å). Such paths give rise to weak scattering in PbCO₃ and Pb(NO₃)₂ in comparison to the same number of SS paths of the same distance. Hence, the <3.5 Å MS paths in Pb(II)EDTA complexes should be weak in comparison to Pb-C SS.

3.5 Pb(II) 3rd Coordination Shell

Pb(II)EDTA²⁻(aq) and all sorption sample spectra contain a substantial third frequency, manifest in the FTs (Fig. 5) as a peak at *ca* 3.6 Å (uncorrected for phase shift), which corresponds to Pb-O distances of 4.2 to 4.3 Å. This distance matches the expected distances to the four EDTA carboxylate O atoms not bonded to Pb(II) (denoted O_{distal}). In Sn(II)EDTA, Sn-O_{distal} = 4.26, 4.48, 4.58, and 4.60 Å. The carboxylate C atoms that bridge between Sn(II)-bonded O and O_{distal} are interposed almost directly between Sn(II) and O_{distal} (*cf.* Fig. 6), giving rise to pseudo-linear Sn-O_{distal}-C-Sn, Sn-C-O_{distal}-Sn, and Sn-C-O_{distal}-C-Sn MS paths. The shortest of these paths has R_{effective} ≥ 4.29 Å. To ascertain whether the 3rd-shell FT peaks could arise from these MS paths, we used their FEFF 6-derived phase and amplitude parameters to fit the sample spectra. Both R_{MS} and CN_{MS} were allowed to float. Figure 8 shows the MS and SS fits to the residual EXAFS spectrum from the 1.8 μmol./m² Pb(II)EDTA/goethite sample. The SS Pb-O_{distal} paths provide substantially better fits to the EXAFS frequencies than do the MS paths, suggesting the 3rd-shell is dominated by Pb-O_{distal} SS.

Both SS and MS 3rd-shell paths arise from, and hence are highly sensitive to, the position (distance) of O_{distal}. Hence, changes in R_{Pb-Odistal} (and possibly CN_{Pb-Odistal}) can be used to infer changes in bonding of the distal carboxylate O atoms for SS or MS. The values of R_{Pb-Odistal} and CN_{Pb-Odistal} for our sorption samples are similar to those for aqueous Pb(II)EDTA²⁻, indicating the distal carboxylate O atoms of the adsorbed complexes have the same structural environment as those in aqueous solution. Hence, they should not be bonded to Fe(III), in agreement with our FTIR results.

4. DISCUSSION

4.1 Outer-Sphere and Hydration-Sphere Adsorption of Pb(II)EDTA on Goethite

Our FTIR and EXAFS results indicate that carboxylate-Fe_{sfc} (“sfc” denotes the specified atom is part of the goethite surface) and Pb-O_{sfc} bonding did not exist in our samples at detectable concentrations and that, in the adsorbed complexes, EDTA acts as a hexadentate ligand to Pb(II). The EXAFS spectra

contain no evidence for inner sphere bonding of Pb(II) to goethite at Pb:EDTA = 1:1. We conclude that inner-sphere bonding of Pb(II)EDTA complexes did not occur to a detectable extent in these samples. Since substantial Pb(II)EDTA²⁻ uptake was observed in the samples, it follows that Pb(II)EDTA complexes should have been adsorbed either as outer-sphere complexes, *i.e.*, retaining their complete aqueous solvation spheres, and/or *via* direct hydrogen bonds to surface functional groups, which displace part of the aqueous solvation shell. There were no major spectral changes as functions of pH, ionic strength, and [PbEDTA]_T. If the complexes had clustered into larger multimetric species, the accompanying changes in structure necessary to bind together anionic complexes, such as EDTA bridging between Pb(II) atoms, should have been detected in both EXAFS and FTIR spectra. Hence, we conclude that clustering of the complexes did not occur.

Several previous studies indicate that Pb(II)EDTA and other Me(II)EDTA complexes exhibit significant positive uptake at $\text{pH} \cdot \text{pH}_{\text{PZC}}$ on both Fe- and Al-oxides. Nowack and Sigg (1996) showed Pb(II)EDTA uptake on goethite at pH 8 (the highest pH for which they measured Pb(II)) compared to a pH_{PZC} of 7.4. Bowers and Huang (1986) showed Pb(II)EDTA uptake on $\gamma\text{-Al}_2\text{O}_3$ up to pH 10 vs. a reported pH_{PZC} of 9.0 to 9.7. Ni(II)EDTA and Co(II)EDTA uptake isotherms are nearly identical to that of Pb(II)EDTA, all other conditions being equal (Bowers and Huang, 1986; Nowack and Sigg, 1996). Nowack and Sigg show Ni(II)EDTA uptake on goethite as high as pH 9, whereas Girvin *et al.* (1993) show that Co(II)EDTA adsorbs on $\gamma\text{-Al}_2\text{O}_3$ at pH 9.5 (isoelectric point reported to be 9.2). In all cases, the authors argued that the complexes should have had composition Me(II)EDTA²⁻. These observations suggest that anionic Me(II)EDTA complexes can adsorb on neutral and/or negatively charged surfaces. This conclusion implies the existence of short-range surface-adsorbate forces such as hydrogen bonding. Others (*e.g.*, Bowers and Huang, (1986) and Girvin *et al.* (1993)) have proposed that Me(II)/(III)EDTA complexes may hydrogen bond to oxide surface sites. Given the donor capacity of the carboxylate oxygens (in adsorbed Pb(II)EDTA complexes) not bonded to Pb(II), it is plausible that hydrogen bonds could form between them and surface (hydr-)oxo groups. This mode of sorption falls between common structural definitions of inner-sphere (*i.e.*, covalently bonded to the oxide surface) and outer-sphere (*i.e.*, adsorbates retain complete shells of solvating water molecules) complexes (Sposito, 1984). Since the chemical potentials and properties of ions are heavily influenced by their distance of approach and bonding to oxide surfaces (Stumm, 1992), a unique designation is warranted to distinguish this mode of hydrogen-bonding sorption from inner- and outer-sphere mechanisms (defined above). Hydrogen-

bonded complexes should occupy space in the primary hydration spheres of surface sites, which otherwise would be filled by solvating water molecules or solute ions. Hence, we propose the name *hydration-sphere* complexes for this mode of adsorption.

Since Pb(II)EDTA uptake is correlated with the density of protonated surface functional groups (Bowers and Huang, 1986), we infer that EDTA methyl H atoms do not form hydrogen bonds to negatively charged surface (hydr)oxo groups (*i.e.*, the chelate does not act as a hydrogen bond donor to surface sites) to an extent sufficient to influence sorptive behavior. Hence, hydration-sphere bonding should be dominated by surface donor/ chelate acceptor hydrogen bonding interactions. The ATR-FTIR spectra provide permissive evidence for the hypothesis that Pb(II)EDTA²⁻ complexes bond to goethite as hydration-sphere complexes. For Pb(II)EDTA complexes adsorbed to goethite, C-O ν_{asym} (1569 cm⁻¹) is shifted to a substantially lower frequency than for Pb(II)EDTA complexes in bulk aqueous solution (C-O ν_{asym} • 1580 cm⁻¹; *cf.*, Fig. 2). Because the C-O ν_{asym} frequency is sensitive to the chemical environment, this peak shift suggests a significant difference between the coordination environments of adsorbed and aqueous Pb(II)EDTA. Since the EXAFS and FTIR spectral features imply the absence of carboxylate- and/or amine-Fe(III) bonding, we attribute this peak shift to hydrogen bonding interactions between goethite surface sites and EDTA carboxylate groups and/or solvation shells of adsorbed complexes, such as proposed by Bargar *et al.* (1996).

Several general conclusions regarding other divalent metal ion EDTA complexes follow from the preceding conclusion. First, our results suggest that Me(II)EDTA complexes can hydrogen bond to oxide surfaces even when all carboxylate arms of EDTA are bonded to the central Me ion. A second conclusion follows from the remarkable (nearly identical) similarity of other Me(II)EDTA (Me = Co, Ni, Cu, Zn) uptake isotherms on goethite and on alumina to those of Pb(II)EDTA on each oxide. Since these complexes have the same charge, the similarity of their uptake isotherms implies that they adsorb *via* the same mechanisms (*i.e.*, outer-sphere and/or hydration-sphere). Therefore, we suggest that adsorbed EDTA complexes of divalent Ni, Cu, Zn, and Co should also reside in the hydration sphere of goethite surfaces sites. Since hydrogen bonding does not directly involve the metal atoms of the oxide substrate, a third conclusion is that all of the above conclusions should hold for sorption on oxides with similar charging behavior. This conclusion is consistent with the results of Bowers and Huang (1986) and Girvin *et al.* (1993). A fourth conclusion regards the dramatically lower sorptive capacity of Fe(III)- and Al(III)-oxides for Co(III)EDTA as compared to Co(II)EDTA (Girvin *et al.*, 1993; Nowack and Sigg, 1996).

Girvin explained the difference in uptake by proposing that quinquidentate Co(II)EDTA complexes hydrogen bond to goethite surface sites more strongly than hexadentate Co(III)EDTA⁻ because the latter did not have a free carboxylate arm. The discussion above suggests that Co(II)EDTA complexes also should have no free carboxylate arms on goethite. Therefore, the difference in uptake should be attributed primarily to the difference in charge of these complexes, and not to the absence of free carboxylate arms. Cases in which Me(II)EDTA complexes exhibit greater uptake than Me(III)EDTA complexes at pH • pH_{pzc}, *e.g.*, Pb(II) *vs.* Co(III) on goethite (Nowack and Sigg, 1996), can be attributed to different partial charges and/or Lewis base strength on carboxylate oxygens, which are influenced by the charge, radius, electronic configuration, and Lewis acidity of cations (Shriver *et al.*, 1990).

4.2 Implications for Surface Complexation Models

Both EXAFS and FTIR results suggest that Pb(II) adsorbate species (observed in this study) had composition Pb(II)EDTA²⁻. There was no evidence for the existence of adsorbed Pb(II)HEDTA⁻ or other protonation states. Hence, adsorption should proceed according to:



where $\equiv\text{FeOH}_2^+$ denotes a structurally undifferentiated, positively charged surface functional group (the number of protons and charge on the site were chosen to be consistent with common descriptions of goethite surface Brönsted acid/base groups, *e.g.*, Bowers and Huang (1996) and Zachara *et al.* (1995)), and " \cdots " denotes outer-sphere and/or hydrogen bond associations to protonated surface functional groups. Based on the similarities of Pb(II)EDTA uptake to those of other Me(II)EDTA complexes, we suggest that reaction (1) should also occur for Co(II)-, Ni(II)-, Cu(II)-, and Zn(II)EDTA adsorption on Fe- and Al-oxides.

4.3 Implications for Goethite Dissolution Mechanisms

Both proton- and (metal-)ligand-promoted mechanisms have been proposed to describe Fe- and Al-oxide dissolution in the presence of metal-EDTA complexes. Szecsody *et al.* (1994) proposed a (metal-)ligand-promoted model in which Me(II)EDTA complexes bond to surface hydroxyl groups (denoted as $\equiv\text{FeOH}_2$) and dissociate to form adsorbed Me(II) ions and outer-sphere Fe_{sf.}-bonded EDTA

complexes, which were proposed to evolve to surface-bound Fe(III)EDTA chelate complexes and then detach from the surfaces. At pH 6.5, the onset of Fe(III)EDTA release into solution was found to lag the onset of EDTA release from dissociated Me(II)EDTA complexes (\bullet 2 h.) by several hundred hours. Thus, a significant concentration of adsorbed outer-sphere EDTA (not bonded to Me(II)) should have accumulated at oxide-water interfaces prior to Fe(III)EDTA release. In our system, such a build-up of adsorbed outer-sphere EDTA should have been detectable and distinguishable from adsorbed Pb(II)EDTA chelate complexes, since the FTIR spectra of these species are different (*cf.*, Fig. 2). The absence of FTIR spectral signatures corresponding to free or Fe(III)-bonded EDTA carboxylate groups suggests that the dissolution-promoting EDTA surface species proposed by Szecsody *et al.* did not occur at significant concentrations in our samples. An alternative explanation for the retarded release of Fe(III) observed by Szecsody *et al.* is that the Fe-oxide dissolution rate was limited by proton-attack mechanisms that are apparently slower than Co(II)EDTA dissociation. This is consistent with the dissolution-rate measurements of Szecsody *et al.* at pH 4.5, which they showed to be consistent with proton-promoted dissolution (as well as metal-ligand-promoted dissolution).

Nowack and Sigg (1996) proposed a Me(II)EDTA-promoted dissolution model in which quinquidentate Me(II)EDTA complexes (*i.e.*, one free carboxylate group) adsorb to $\equiv\text{Fe}_{\text{sfc}}$ sites *via* inner-sphere bonding between the free carboxylate group and surface Fe atoms, followed by opening of the EDTA ring and simultaneous bonding of EDTA as a tridentate iminodiacetate ligand to each goethite surface Fe atoms and adsorbed Me(II) ions. Formation of these activated complexes (denoted herein as Pb(II)EDTA- Fe_{sfc}) was proposed to be the rate-determining step. Fe(III) detachment was thought to follow dissociation of the remaining Me(II)-EDTA bonds. The proposed precursor complexes should be observable by spectroscopic methods, since they exist at detectable concentrations for periods of hours to weeks before being consumed. However, we observed no such species, even though dissolution should have reached steady state. These observations suggest at least one of the following conclusions: (1) the dissolution rate of goethite in the presence of Pb(II)EDTA is controlled by proton-promoted dissolution, and inner-sphere EDTA- Fe_{sfc} species did not occur; (2) the inner-sphere Pb(II)EDTA- Fe_{sfc} precursor complexes of Nowack and Sigg existed at very low (undetectable) concentrations in our samples; (3) the outer-sphere complexes observed in our samples were precursors to Nowack and Sigg's Pb(II)EDTA- Fe_{sfc} precursor species, and the rate of formation of the latter complexes was very slow and/or rate determining (in which case Nowack and Sigg's Pb(II)EDTA- Fe_{sfc} precursor species would be difficult to detect

spectroscopically because they would be consumed as quickly as they were formed); (4) the outer-sphere complexes observed in our samples were immediate precursors to iminodiacetate activated complexes.

Bryce *et al.* (1994) have argued that closure of the EDTA chelate *via* formation of amine-Me(II) bonds (as opposed to bonding by a carboxylate group) should be the rate-determining step for ferrihydrite (hydrated Fe(III)-oxide) dissolution in the presence of Ni(II)EDTA, based on comparison to the reaction rates in bulk aqueous solution. This argument suggests that scenario (3) above is unlikely, since it requires that formation of EDTA carboxylate-Fe_{sc} bonds be as slow or slower than ring closure around Fe(III). Suggestion (2) above implies that the concentrations of inner-sphere bonded Pb(II)EDTA-Fe_{sc} precursor complexes should not in general be directly related to the macroscopically measured adsorption density (which is dominated by hydration-sphere bonded complexes), since the reaction stoichiometries of inner-sphere and hydration-sphere adsorption reactions are likely to differ substantially. Furthermore, if the precursor complexes form quickly (as proposed by Nowack and Sigg and as necessitated by the very low concentration of the species), they should be in equilibrium with bulk solution, since many of the possible routes to their formation are faster. Hence, rate constants for the explicitly described dissolution mechanisms determined using macroscopically measured adsorption densities may be inaccurate, particularly when extrapolated to solution conditions different from those used to calibrate the model.

5 SUMMARY AND CONCLUSIONS

ATR-, DR-FTIR, and EXAFS spectra of Pb(II)EDTA adsorbed on goethite are similar to the corresponding spectra of aqueous Pb(II)EDTA²⁻, indicating an intact chelate complex on goethite, with 4 carboxylate and 2 amine groups bonded to Pb(II), at all conditions examined in this study (pH 4 - 6, [Pb(II)EDTA]_T = 0.014 to 2.7 mM, 0.8 mM to 0.5 M ionic strength, varying electrolytes). EXAFS analysis suggests the Pb(II)-O coordination shell is composed of 6 O/N atoms at 2.45 to 2.5 Å and an additional 1 to 2 water molecules at about 3.3 Å. No evidence for bonding between EDTA molecules and surface Fe atoms was observed in any samples, nor were any vibrational frequencies corresponding to protonated carboxylate groups. Since EXAFS and FTIR spectra of Pb(II)EDTA adsorbed on goethite are similar to the corresponding spectra of aqueous Pb(II)EDTA²⁻, we conclude that the complexes had composition Pb(II)EDTA²⁻.

Comparison of the FTIR and EXAFS results to the uptake characteristics of Pb(II)EDTA²⁻ on goethite suggests that Pb(II)EDTA²⁻ adsorption is consistent with outer-sphere complexes and/or a hydrogen bonding mechanism in which carboxylate oxygens on the chelate complex directly hydrogen bond to protonated surface functional groups, displacing waters of solvation from PbEDTA(II)²⁻. Since complexes adsorbed according to this latter mechanism occupy space next to goethite surface functional groups, which would otherwise be occupied by solvating water molecules, we designate them as hydration-sphere complexes. These results suggest that Me(II)EDTA complexes having no free carboxylate arms can participate in hydrogen bonding interactions with oxide surfaces. Metal-ligand-promoted dissolution models should be modified to account for the existence of outer-sphere and/or hydration-sphere complexes. Based on the current results and the striking similarity of Co(II)-, Ni(II)-, Cu(II), and Zn(II)-EDTA uptake isotherms to those for Pb(II)EDTA, we propose that Co(II)-, Ni(II)-, Cu(II), and Zn(II)EDTA adsorbed on goethite and alumina should not have free carboxylate arms and hence should be predominantly outer- or hydration-sphere complexes.

Acknowledgments - We thank Sandy Robertson for providing the goethite sample used in this study, the staff of the Stanford Synchrotron Radiation Laboratory (SSRL), particularly Britt Hedman, for their help and advice, and three anonymous reviewers for their helpful comments. We acknowledge the U.S. Department of Energy for funding this work through grant DE-FG03-93ER14347. SSRL is supported by the Department of Energy, Office of Basic Energy Sciences under SLAC contract number DE-AC03-76SF00515. We also acknowledge the National Institutes of Health, National Center for Research Resources, Biomedical Technology Program, and the DOE Office of Biological and Environmental Research, which support SSRL.

REFERENCES

- Bargar J. R., Brown G. E., Jr., and Parks G. A. (1997a) Surface complexation of Pb(II) at oxide-water interfaces: I. XAFS and bond-valence determination of mono- and polynuclear Pb(II) sorption products on Al-oxides. *Geochim. Cosmochim. Acta* **61**, 2617-2638.
- Bargar J. R., Brown G. E., Jr., and Parks G. A. (1997b) Surface complexation of Pb(II) at oxide-water interfaces: II. XAFS and bond-valence determination of mononuclear Pb(II) sorption products and surface functional groups on Fe-oxides. *Geochim. Cosmochim. Acta* **61**, 2639-2652.

- Bargar J. R., Brown G. E., Jr., and Parks G. A. (1998) Surface complexation of Pb(II) at oxide-water interfaces: III. XAFS determination of Pb(II) and Pb(II)-chloro adsorption complexes on goethite and alumina. *Geochim. Cosmochim. Acta* **62**, 193-207.
- Bargar J. R. and Persson P. (1999) Outer-sphere adsorption of EDTA on goethite. *J. Colloid Interf. Sci.*, in submission.
- Bargar J. R., Reitmeyer R. L., and Davis J. A. (1999) Spectroscopic characterization of U(VI)-carbonato surface complexes on hematite and ferrihydrite. In *Surface Complexation Modeling of U(VI) Adsorption on Natural Mineral Assemblages. NUREG Report.*, pp. In Press. U.S. Nuclear Regulatory Commission.
- Bargar J. R., Towle S. N., Brown G. E., Jr., and Parks G. A. (1996) Outer-sphere lead(II) adsorbed at specific surface sites on single crystal α -alumina. *Geochim. Cosmochim. Acta* **60**, 3541 - 3548.
- Bargar J. R., Towle S. N., Brown G. E., Jr., and Parks G. A. (1997c) XAFS and bond-valence determination of the structures and compositions of surface functional groups and Pb(II) and Co(II) sorption products on single-crystal α -Al₂O₃. *J. Coll. Interf. Sci.* **185**, 473-492.
- Blaylock M. J., Salt D. E., Dushenkov S., Sakharova O., Gussman C., Kapulnik Y., B.D. Ensley, and Raskin I. (1997) Enhanced accumulation of Pb in Indian mustard by soil-applied chelating agents. *Environ. Sci. Technol.* **31**, 860-865.
- Bowers A. R. and Huang C. P. (1986) Adsorption characteristics of metal-EDTA complexes onto hydrous oxides. *J. Coll. Interf. Sci.* **110**, 575-590.
- Bryce A. L., Kornicker W. A., and Clark S. B. (1994) Nickel adsorption to hydrous ferric oxide in the presence of EDTA: Effects of component addition sequence. *Environ. Sci. Technol.* **28**, 2353-2359.
- Busch D. H. and J.C. Bailar J. (1953) The stereochemistry of complex inorganic compounds XVII. The stereochemistry of hexadentate ethylenediaminetetraacetic acid complexes. *J. Amer. Chem. Soc.* **75**, 4574-4575.
- Chisholm-Brause C. J., Hayes K. F., Roe L. A., Brown G. E., Jr., G.A. Parks, and Leckie J. O. (1990) Spectroscopic investigation of Pb(II) complexes at the γ -Al₂O₃/water interface. *Geochim. Cosmochim. Acta* **54**, 1897-1909.
- Erel Y. and Morgan J. J. (1992) The relationships between rock-derived lead and iron in natural waters. *Geochim. Cosmochim. Acta* **56**, 4157 - 4167.
- Fujita J., Martell A. E., and Nakamoto K. (1962) Infrared spectra of metal chelate compounds. VI. A normal coordinate treatment of oxalato metal complexes. *J. Chem. Phys.* **36**, 324-338.
- George G. N. (1993) EXAFSPAK. Stanford Synchrotron Radiation Laboratory.
- Girvin D. C., Gassman P. L., and H. Bolton J. (1993) Adsorption of aqueous cobalt ethylenediaminetetraacetate by γ -Al₂O₃. *Soil Sci. Soc. Am. J.* **57**, 45-57.

- Greenwood N. N. and Earnshaw A. (1985) *Chemistry of the Elements*. Pergamon Press.
- Gunneriusson L., Lovgren L., and Sjöberg S. (1994) Complexation of Pb(II) at the goethite (α -FeOOH)/water interface: The influence of chloride. *Geochim. Cosmochim. Acta* **58**, 4973-4983.
- Harrison P. G., Healy M. A., and Steel A. T. (1982) EDTA-chelation therapy of lead poisoning: lead-207 nuclear magnetic resonance and x-ray diffraction studies. *Inorg. Chim. Acta* **67**, L15-L16.
- Harrison P. G. and Steel A. T. (1982) Lead(II) carboxylate structures. *J. Organometallic Chem.* **239**, 105-113.
- Hem J. D. (1976) Geochemical controls on lead concentrations in stream water and sediments. *Geochim. Cosmochim. Acta.* **40**, 599 - 609.
- Huang J. W., Chen J., Berti W. B., and Cunningham S. D. (1997) Phytoremediation of lead-contaminated soils: role of synthetic chelates in lead phytoextraction. *Environ. Sci. Technol.* **31**, 800-805.
- Huang J. W. and Cunningham S. D. (1996) Lead phytoextraction: species variation in lead uptake and translocation. *New Phytol.* **134**, 75-84.
- Jardine P. M., Jacobs G. K., and O'Dell J. D. (1993) Unsaturated transport processes in undisturbed heterogeneous porous media: II. Co-contaminants. *Soil Sci. Soc. Am. J.* **57**, 954-962.
- Jenne E. A. (1967) Controls on Mn, Fe, Co, Ni, Cu and Zn concentrations in soils and water: the significant role of hydrous Mn and Fe oxides. In *Trace Inorganics in Water*, Vol. 73, pp. 337 - 387. American Chemical Society.
- Jørgensen S. E. (1993) Removal of heavy metals from compost and soil by echotechnological methods. *Ecol. Eng.* **2**, 89-100.
- Kari F. G. and Giger W. (1995) Modeling the photochemical degradation of EDTA in the river Glatt. *Environ. Sci. Technol.* **29**, 2814-2827.
- Krishnan K. and Plane R. A. (1968) Raman spectra of ethylenediaminetetraacetic acid and its metal complexes. *J. Amer. Chem. Soc.* **90**, 3195-3199.
- Manceau A., Charlet L., Boisset M. C., Didier B., and Spadini L. (1992) Sorption and speciation of heavy metals on hydrous Fe and Mn oxides. From microscopic to macroscopic. *Applied Clay Sci.* **7**, 201-230.
- McConnell A. A. and Nuttall R. H. (1977) the vibrational spectra of EDTA complexes of divalent tin and lead. *Spectrochim. Acta* **33A**, 459-462.
- Means J. L., Kucak T., and Crerar D. A. (1980) Relative degradation rates of NTA, EDTA, and DTPA and environmental implications. *Environ. Poll.* **1**, 45-60.
- Morris M. L. and Busch D. H. (1956) The properties and infrared absorption spectra of complexes of cobalt(III) with pentadentate ethylenediaminetetraacetic acid and hydroxyethylenediaminetriacetic acid. *J. Amer. Chem Soc.* **78**, 5178-5181.
- Nakamoto K. (1986) *Infrared and Raman Spectra of Inorganic and Coordination Compounds*. J. Wiley and Sons.

- Nakamoto K., Morimoto Y., and Martell A. E. (1963) Infrared spectra of aqueous solution. III. ethylenediaminetetraacetic acid, N-hydroxyethylenediaminetriacetic acid, and diethylenetriaminepentaacetic acid. *J. Amer. Chem. Soc.* **85**, 309-316.
- Nordin J., Persson P., Laiti E., and S. Sjöberg. (1997) Adsorption of o-phthalate at the water-boehmite (γ -AlOOH) interface: Evidence for two coordination modes. *Langmuir* **13**, 4085-4083.
- Nordin J., Persson P., Nordin A., and Sjöberg S. (1998) Inner- and outer-sphere complexation of a polycarboxylic acid at the water-boehmite (γ -AlOOH) interface: A combined potentiometric and IR spectroscopic study. *Langmuir* **14**, 3655-3662.
- Nowack B. and Sigg L. (1996) Adsorption of EDTA and metal-EDTA complexes onto goethite. *J. Colloid Interf. Sci.* **177**, 106-121.
- Nowack B. and Sigg L. (1997) Dissolution of Fe(III)(hydr)oxides by metal-EDTA complexes. *Geochim. Cosmochim. Acta* **61**, 951-963.
- Persson P., Karlsson M., and Ohman L.-O. (1998a) Coordination of acetate to Al(III) in aqueous solution and at the water-aluminum hydroxide interface: A potentiometric and attenuated total reflectance FTIR study. *Geochim. Cosmochim. Acta*, in press.
- Persson P., Nordin J., Rosenqvist J., Lovgren L., Ohman L.-O., and Sjöberg S. (1998b) Comparison of the adsorption of o-phthalate on boehmite, aged γ -Al₂O₃, and goethite. *J. Coll. Interf. Sci.* **206**, 252-256.
- Reed G. H. and Kula R. J. (1971) Nuclear magnetic resonance and infrared spectral studies of structural and kinetic properties of amino polycarboxylate chelates of divalent lead, zinc, cadmium, and mercury in acidic aqueous solution. *Inorg. Chem.* **10**, 2050-2057.
- Rehr J. J. and Albers R. C. (1990) Scattering-matrix formulation of curved-wave multiple-scattering calculations of X-ray absorption fine structure. *Phys. Rev. B* **41**, 8139-8149.
- Rehr J. J., Mustre de Leon J., Zabinsky S. I., and Albers R. C. (1991) Theoretical x-ray absorption fine structure standards. *J. Amer. Chem. Soc.* **113**, 5135-5140.
- Rehr J. J., Zabinsky S. I., and Albers R. C. (1992) High-order multiple-scattering calculations of x-ray absorption fine structure. *Phys. Rev. Lett.* **69**, 3397.
- Roe A. L., Hayes K. F., Chisholm-Brause C. J., G.E. Brown J., Parks G. A., Hodgson K. O., and Leckie J. O. (1991) In-situ X-ray absorption study of lead ion surface complexes at the goethite-water interface. *Langmuir* **7**, 367-373.
- Rojo T., Insausti M., Arriortua M. I., Hernandez E., and Zubillaga J. (1992) Thermal decomposition study of some complexes, precursors of mixed oxides, with formula MM'(L)•nH₂O. *Thermochim. Acta* **195**, 94-104.

- Sawer D. T. and Tackett J. E. (1963) Properties and infrared spectra of ethylenediaminetetraacetic acid complexes: V. Bonding and structure of several metal chelate complexes. *J. Amer. Chem. Soc.* **85**, 2390-2394.
- Scott K. L., Wieghardt K., and Sykes A. G. (1973) μ -Oxalato-cobalt(III) complexes. *Inorg. Chem.* **12**, 655-663.
- Shields K. G., Seccombe R. C., and Kennard C. H. L. (1973) Stereochemistry of flexible-chelate-metal complexes. Part III. Crystal structure of dihydrogen ethylenediaminetetra-acetatostannate(II). *J. Chem. Soc. Dalton Transactions*, 741-743.
- Shriver D. F., Atkins P. W., and Langford C. H. (1990) *Inorganic Chemistry*. W.H. Freeman.
- Sievers R. E. and J.C. Bailar J. (1962) Some metal chelates of ethylenediaminetetraacetic acid, diethylenetriaminepentaacetic acid, and triethylenetetraaminehexaacetic acid. *Inorg. Chem.* **1**, 174-182.
- Sposito G. (1984) *The Surface Chemistry of Soils*. Oxford University Press.
- Stumm W. (1992) *Chemistry of the Solid-Water Interface*. J. Wiley.
- Szecsody J. E., J.M. Achara, and Bruckhart P. L. (1994) Adsorption-dissolution reactions affecting the distribution and stability of Co(II)EDTA in iron oxide-coated sand. *Environ. Sci. Technol.* **28**, 1706-1716.
- Van Geen A., Robertson A. P., and Leckie J. O. (1994) Complexation of carbonate species at the goethite surface: Implications for adsorption of metal ions in natural waters. *Geochim. Cosmochim. Acta* **58**, 2073-2086.
- van Remoortere F. P., Flynn J. J., Boer F. P., and North P. P. (1971) The crystal structure of distannous ethylenediaminetetraacetate dihydrate. *Inorg. Chem.* **10**, 1511-1518.
- Yugeng Z. (1993) Structure-chemical study on $\text{Pb}[\text{Co}(\text{HEDTA})\text{H}_2\text{O}]_2 \cdot 4\text{H}_2\text{O}$ crystal. *Cryst. Res. Technol.* **28**, K49-K53.
- Zachara J. M., Smith S. C., and Kuzel L. S. (1995) Adsorption and dissociation of Co-EDTA complexes in iron oxide-containing subsurface sands. *Geochim. Cosmochim. Acta* **59**, 4825-4844.

Table 1. Final sample conditions. $[\text{Pb}]_{\text{T}}:[\text{EDTA}]_{\text{T}} = 1:1$ unless noted otherwise. $[\text{PbL}]_{\text{T}}$ is the total concentration of adsorbed and dissolved Pb(II)EDTA species in solution. $[\text{PbL}]_{\text{eq}}$ is the final concentration of all dissolved Pb(II)EDTA species. *This sample had $[\text{Pb}]_{\text{T}}:[\text{EDTA}]_{\text{T}} = 2:1$.

Method	pH	electrolyte (molarity)	Sorption		solid:liqui d (g/L)	
			Density ($\mu\text{mol./m}^2$)	$[\text{PbL}]_{\text{T}}$ (μM)		
ATR-FTIR	4.01	0.01 NaCl	0.51	137.5	14.70	5.4
ATR-FTIR	4.05	0.01 NaClO ₄	0.53	137.5	9.50	5.4
ATR-FTIR	4.13	0.5 NaCl	0.27	137.5	72.10	5.4
ATR-FTIR	5.06	0.01 NaCl	0.54	137.5	5.80	5.4
ATR-FTIR	5.99	0.01 NaCl	0.49	137.5	18.40	5.4
DR-FTIR	4.03	.01 NaCl	0.09	24.9	2.60	5.3
DR-FTIR	4.04	.01 NaCl	0.50	127.8	5.00	5.4
DR-FTIR	4.04	.01 NaCl	1.01	252.7	9.00	5.3
DR-FTIR	4.97	.01 NaCl	0.06	13.5	0.11	5.4
DR-FTIR	5.05	.01 NaCl	0.11	27.5	0.30	5.5
DR-FTIR	5.03	.01 NaCl	0.55	135.1	1.75	5.4
DR-FTIR	5.06	.01 NaCl	0.98	267.4	31.60	5.3
DR-FTIR	5.08	.01 NaNO ₃	0.93	266.3	43.20	5.3
DR-FTIR	5.03	No Control	1.07	267.0	8.80	5.3
DR-FTIR	6.01	.01 NaCl	0.20	47.4	0.98	5.2
DR-FTIR	5.99	.01 NaCl	0.83	239.6	42.00	5.3
EXAFS	5.04	.01 NaNO ₃	0.88	178.0	17.30	4.0
EXAFS	5.04	.01 NaNO ₃	1.11	848.0	598.00	5.0
EXAFS	5.03	.01 NaNO ₃	1.84	2716.0	2300.00	5.0
EXAFS	5.04	.01 NaNO ₃	3.0	800.0*	262.50	5.0

Table 2. EXAFS fit results. CN = coordination number, R = interatomic distance, σ^2 = Debye-Waller factor (\AA^2), and Γ = sorption density ($\mu\text{mol./m}^2$). Accuracies of R are estimated to be $\pm 0.03 \text{ \AA}$ for all shells. Accuracies of CN are estimated to be $\pm 20\%$ for Pb-O and Pb-N, and $\pm 30\%$ for Pb-C. Least squares precisions are given in parentheses. * This variable was fixed during fits (*cf.*, section 2.4). † Data are from Bargar et al. (1997).

Sample	<u>Pb-O</u>			<u>Pb-N</u>			<u>Pb-C</u> ($\sigma^2 = .013$)		<u>Pb-O_{distal}</u> ($\sigma^2 = .012$)	
	CN	R(\AA)	σ^2	CN	R(\AA)	σ^2	CN	R(\AA)	CN	R(\AA)
pH 5.04 Γ 0.88 1:1 Pb:EDTA	3.5 (0.6)	2.53 (.009)	0.011 (.003)	2.0*	2.38 (.018)	0.011*	8.2 (0.4)	3.32 (.008)	4.7 (.40)	4.25 (.010)
pH 5.04 Γ 1.11 1:1 Pb:EDTA	3.8 (0.4)	2.53 (.005)	0.013 (.002)	2.0*	2.41 (.019)	0.013*	8.9 (0.3)	3.31 (.007)	5.4 (0.4)	4.24 (.007)
pH 5.03 Γ 1.84 1:1 Pb:EDTA	3.8 (0.3)	2.52 (.005)	0.014 (.002)	2.0*	2.41 (.020)	0.014*	8.7 (0.3)	3.31 (.005)	4.9 (0.3)	4.24 (.006)
Pb(II)EDTA ²⁻ (aq)	4.9 (0.4)	2.51 (.005)	0.018 (.001)	2.0*	2.47 (.018)	0.018*	9.0 (0.4)	3.31 (.006)	4.7 (0.4)	4.23 (.008)
pH 6.02 Γ 4.0 No EDTA†	2.4 (0.8)	2.27 (.009)	0.01	.2 Fe (0.1)	3.36 (.035)	0.01	--	--	--	--

FIGURE CAPTIONS

Figure 1. Pb(II)EDTA uptake on goethite at pH 5. Open circles are DR-FTIR data points (0.01 M NaCl), and open squares are EXAFS data points (0.01 M NaNO₃). Nonsystematic error on data points is $\pm 6\%$.

Figure 2. ATR-FTIR spectra of Pb(II)EDTA/ goethite as a function of pH. $\Gamma =$ has units of $\mu\text{mol./m}^2$. Shaded regions give the reported range of C-O ν_{asym} frequencies for carboxylate-Fe(III) and -Pb(II) bonding. Dashed lines give fits to spectra. Pb(II)EDTA²⁻ and Fe(III)EDTA⁻ are from 1:1, 20 mM solutions at pH 6, whereas H₂EDTA²⁻ is 50 mM, pH 4.

Figure 3. Normalized spectra of Pb(II)EDTA/ goethite as a function of Pb(II)EDTA concentration at pH 5. Dashed lines indicate fitted contributions from contaminant carbonate adsorbate species. The small, narrow peak at about 1380 cm⁻¹ is due to trace nitrate contamination.

Figure 4. Normalized ATR- and DR-FTIR spectra of Pb(II)EDTA/goethite in differing electrolytes of ionic strength and composition. The extra amplitude in the 0.01 M NaNO₃ spectrum at *ca.* 1390 cm⁻¹ is due to the presence of nitrate ν_3 frequencies.

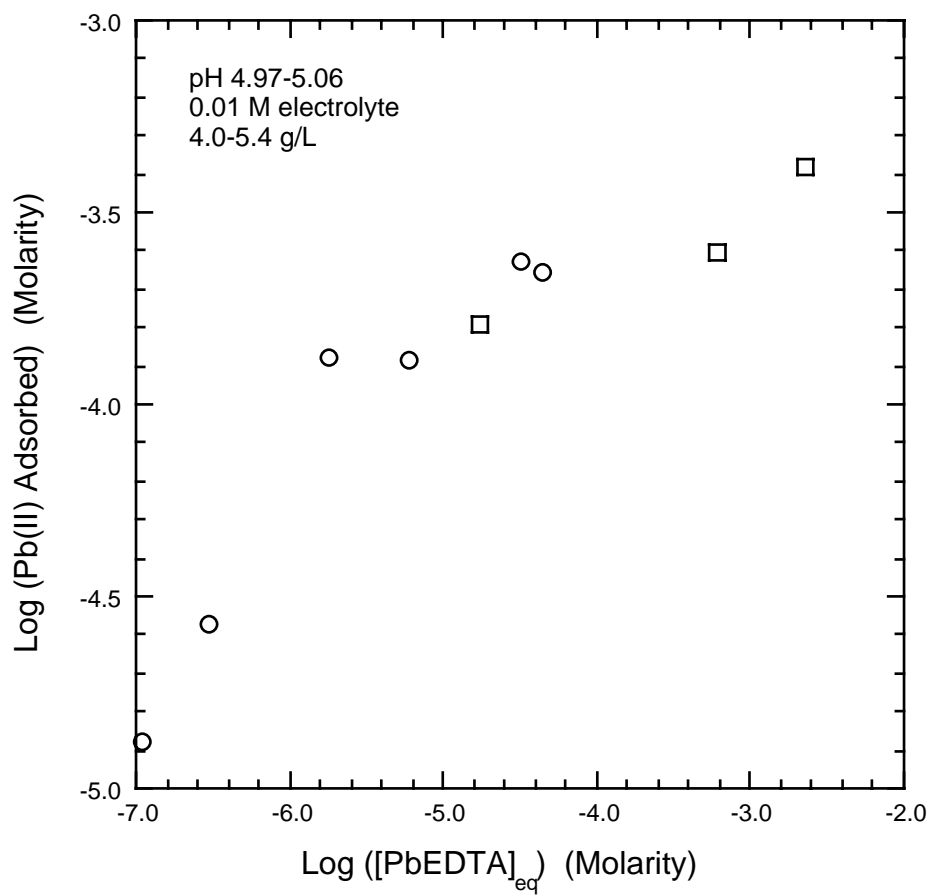
Figure 5. EXAFS spectra and Fourier Transforms (FTs) of Pb(II)EDTA/goethite at pH 5. Dashed lines are fits to spectra. The “No EDTA” sample is from Bargar *et al.* (1998a). The fit to “2:1 Pb:EDTA” is a linear combination of the unsmoothed, background-subtracted, splined, k^3 -weighted EXAFS of “ $\Gamma=1.8 \mu\text{mol./m}^2$ ” (57% contribution) and “No EDTA” (43% contribution), obtained by least-squares fitting. Only % contribution of components were varied in fits.

Figure 6. Structure of Sn(2) site in Sn₂EDTAx2H₂O (van Remoortere *et al.*, 1971).

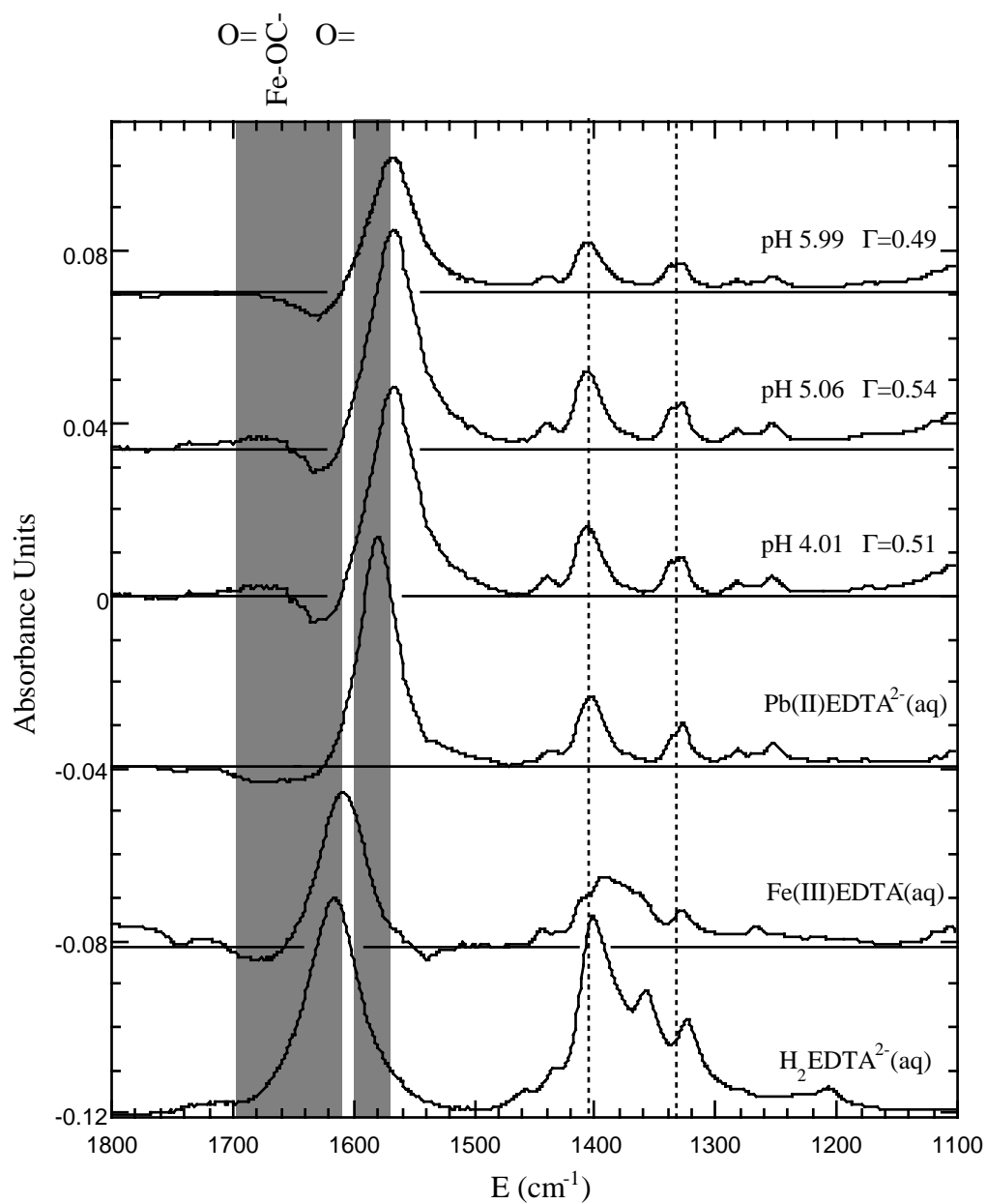
Figure 7. Pb-O bond length ($R_{\text{Pb-O}}$) vs. coordination number (CN) of Pb(II) environments in oxides, hydroxides, and oxysalts. Solid circles give *average* Pb-O bond lengths and were fit to data between $5 \cdot \text{CN} \cdot 12$ (dashed line, correlation coefficient = 0.94), as described in Bargar *et al.* (1997a). Minimum Pb-O bond lengths for each Pb(II) coordination environment (dotted line, correlation coefficient = 0.86) were fit between $2 \cdot \text{CN} \cdot 12$.

Figure 8. Comparison of SS and MS fits (dashed lines) to EXAFS 3rd-shell frequency. Solid lines are residuals from spline-fit k^3 -weighted spectrum of the pH 5, $1.8 \mu\text{mol./m}^2$ sample after subtraction of the lower shells.

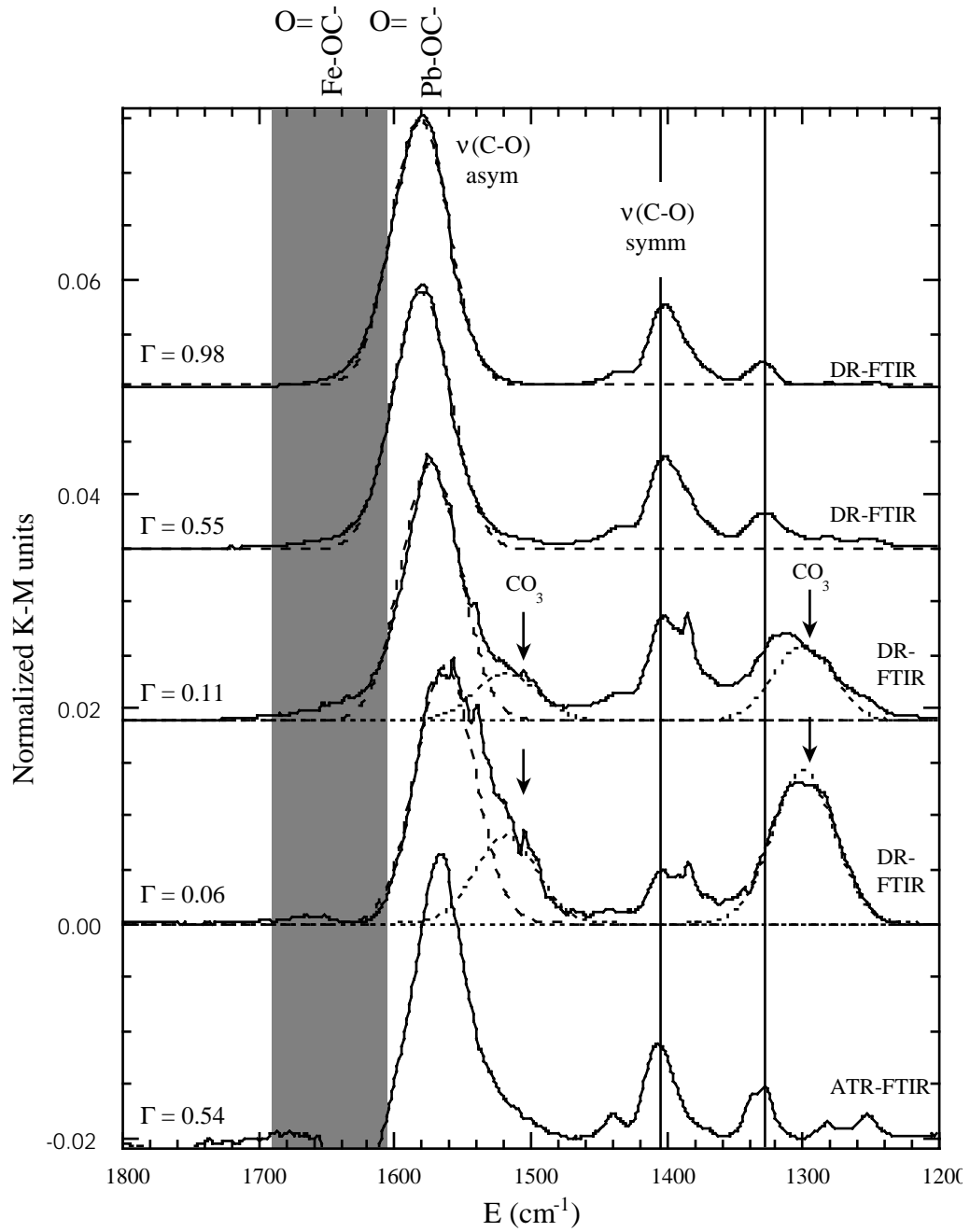
Bargar et al. FIGURE 1.



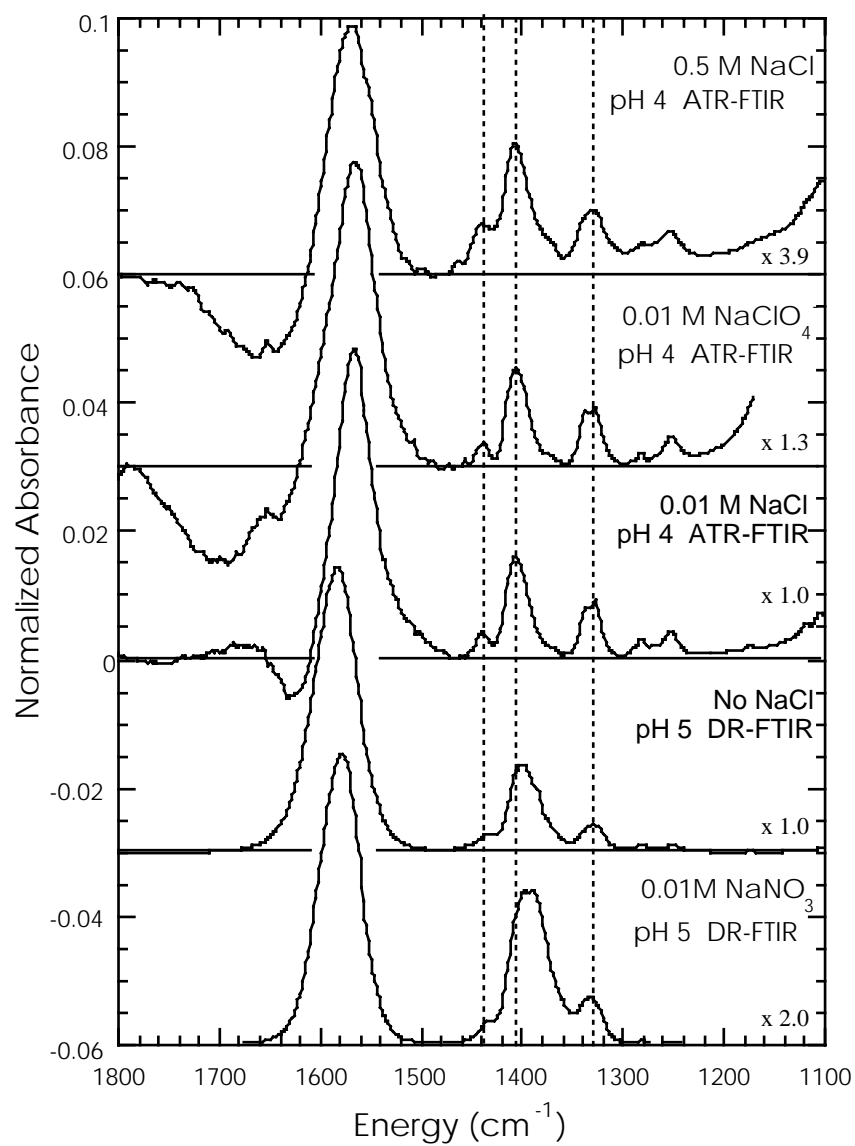
Bargar et al. FIGURE 2.



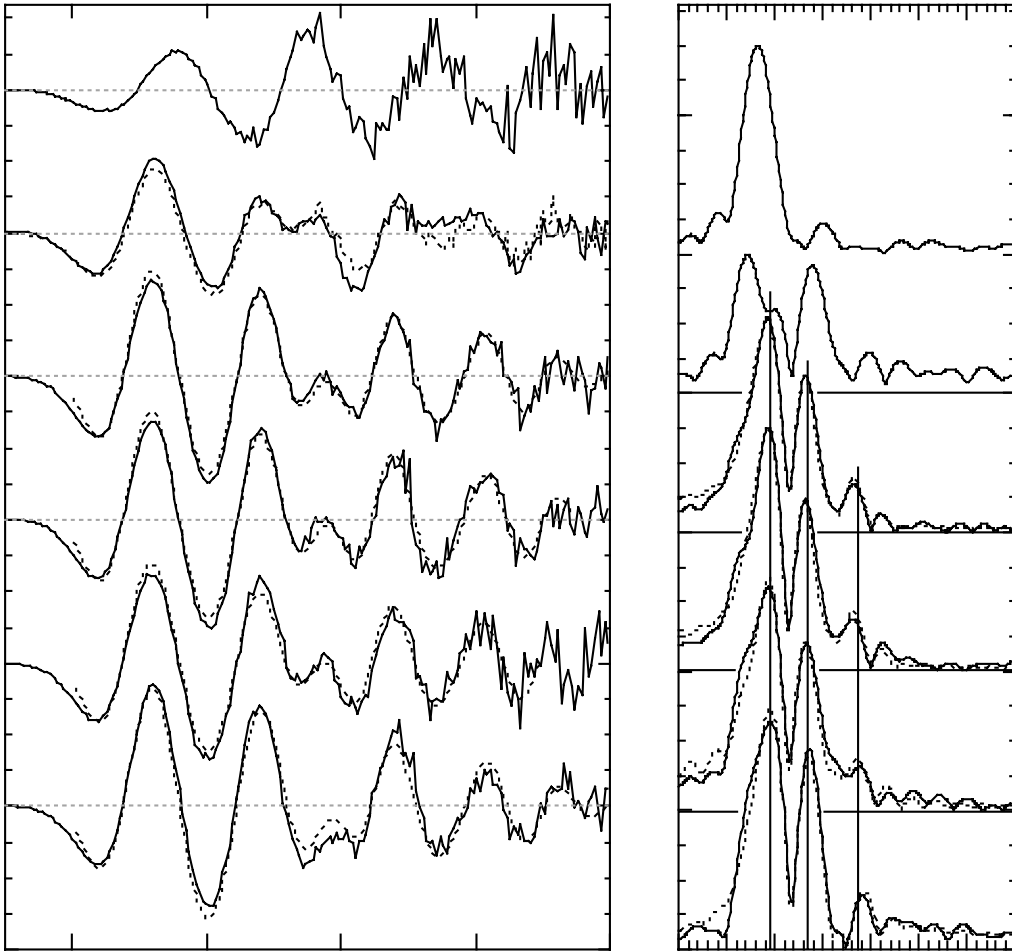
Bargar et al. FIGURE 3.

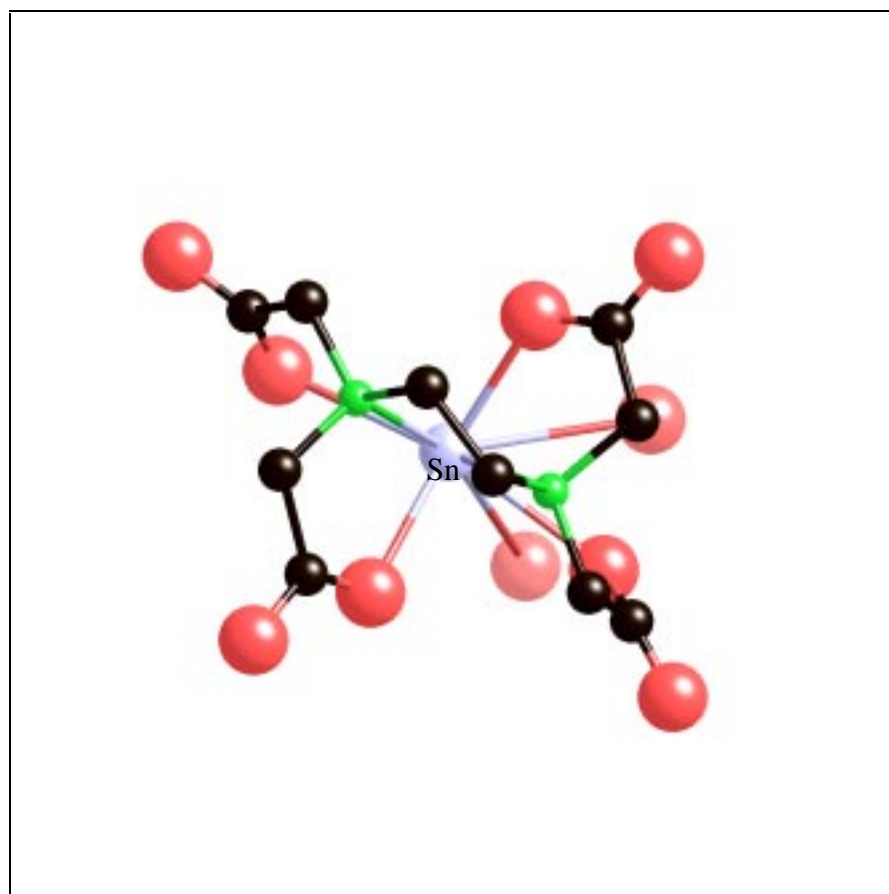


Bargar et al. FIGURE 4.

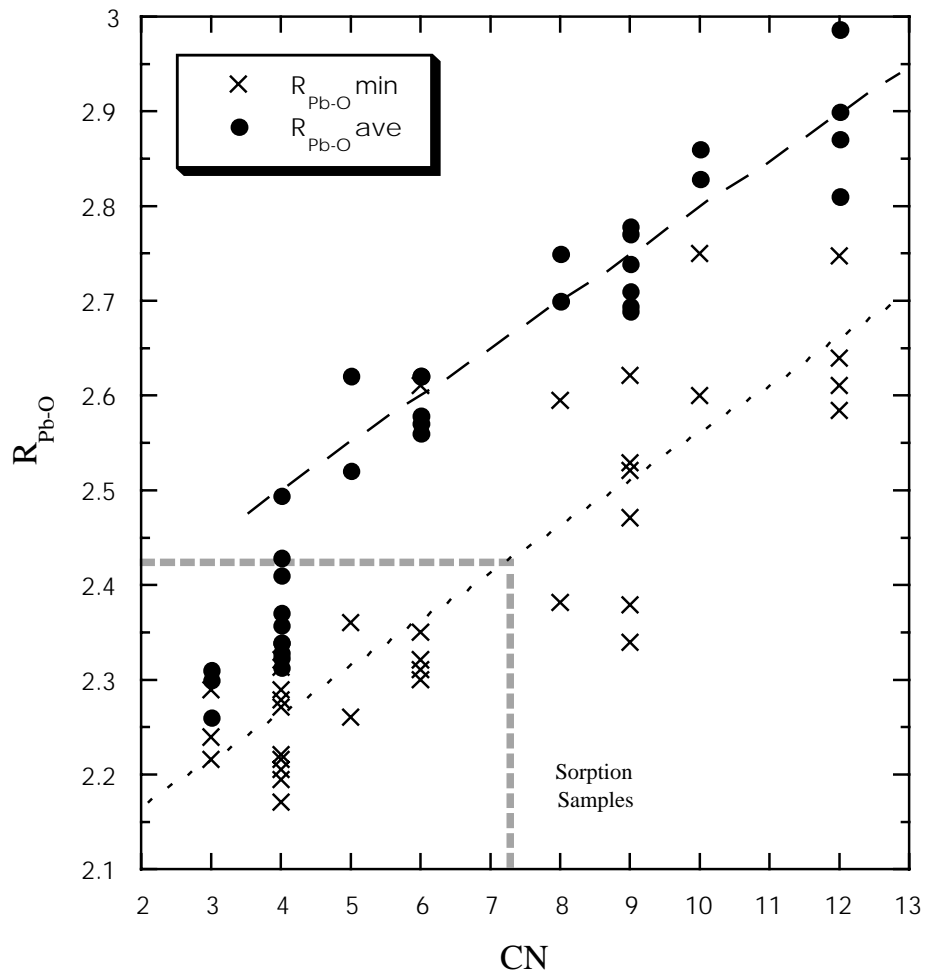


Bargar et al. FIGURE 5.





Bargar et al. FIGURE 7.



Bargar et al. FIGURE 8.

